Modelling ice sheets and ice shelves

Karthaus Summer School 2023

Frank PATTYN

Laboratoire de Glaciologie
Université libre de Bruxelles, Belgium
Frank.Pattyn@ulb.be

May 23, 2023

Numerical modelling of ice sheets and ice shelves

1. Commonly used approximations in ice flow modelling
2. Numerical modelling of ice sheets (SIA)
3. Numerical modelling of marine ice sheets (SSA)

Aim of the course

FOCUS

- Focus on approximations of ice flow
- Numerical approach emphasized

Reference Material

Course material (slides + handouts) and model codes available on `https://github.com/FrankPat/Karthaus`

What is covered during the course?

- Continuum models
- Solving mass continuity equation
- Shallow-ice models
- Shallow-shelf models
- Grounding line migration

Numerical approaches

- Finite difference schemes
- Solving stress balance system
- Verification experiments

References

Books

- Greve, R. and H. Blatter (2009) *Dynamics of ice sheets and glaciers.* Advances in Geophysics and Environmental Mechanics and Mathematics. Springer
- Fowler, A. and F. Ng (2020) Glaciers and Ice Sheets in the Climate System (The Karthaus Summer School Lecture Notes). Springer. doi: 10.1007/978-3-030-42584-5.
- Van der Veen, C. J. 1999. *Fundamentals of Glacier Dynamics.* A. A. Balkema, Rotterdam.

Articles

- Docquier, D., L. Perichon, F. Pattyn (2011) Representing grounding line dynamics in numerical ice sheet models: Recent advances and outlook. Surveys in Geophysics. doi:10.1007/s10712-011-9133-3
- Pattyn, F. (2003) A new three-dimensional higher-order thermomechanical ice sheet model: basic sensitivity, ice stream development and ice flow across subglacial lakes. Journal of Geophysical Research (Solid Earth), 108 (B8), 2382, doi:10.1029/2002JB002329
- Pattyn, F. et al. (2012) Results of the Marine Ice Sheet Model Intercomparison Project, MISMIP. The Cryosphere, 6, 573-588, doi:10.5194/tc-6-573-2012
- Pattyn, F. (2017) Sea-level response to melting of Antarctic ice shelves on multi-centennial timescales with the fast Elementary Thermomechanical Ice Sheet model (f.ETISh v1.0), The Cryosphere, 11, 1851-1878
- Pattyn, F. (2018) The paradigm shift in Antarctic ice sheet modelling. Nature Communications 9 (2728).
- Pattyn, F. and Morlighem, M. (2020) The uncertain future of the Antarctic Ice Sheet. Science 367(6484): 1331-1335.

Numerical modelling of ice sheets and ice shelves

1. **Commonly used approximations in ice flow modelling**
   - Stokes equations
   - Approximations to the Stokes equations (FS)
   - Blatter–Pattyn models (LMLa)
   - Shallow shelf approximations (SSA or L1L1)
   - Shallow ice approximation (SIA or S)
   - Hybrid models
   - Ice-sheet evolution
   - Applicability of approximations
2. Numerical modelling of ice sheets (SIA)
3. Numerical modelling of marine ice sheets (SSA)

Ice flow: Kinematics *vs* Dynamics

Kinematic description of ice flow

- Steady – transient state
- Flow is what it needs to be, to carry away upstream accumulation.
- Glacier has adjusted its shape to make this flow happen.

Dynamic description

- Ice is a material with certain rheological properties (stiffness).
- Flow is determined by forces (stresses) applied to it.

Both descriptions are needed

- Rheological properties don't figure in kinematic description.
- Accumulation and ablation don't figure in dynamic description.

Field equations

Conservation of mass is described by the continuity equation,

$$\frac{\mathrm{d}\rho}{\mathrm{d}t} + \nabla \cdot (\mathbf{v}\rho) = 0 \tag{1}$$

- ρ is the density
- $\mathbf{v}$ is the velocity vector

This can be reduced to the incompressibility condition,

$$\nabla \cdot \mathbf{v} = 0 \tag{2}$$

Conservation of linear momentum:

$$\rho \frac{\mathrm{d}\mathbf{v}}{\mathrm{d}t} = \nabla \cdot \boldsymbol{\sigma} - \rho \mathbf{g} \tag{3}$$

- $\boldsymbol{\sigma}$ is the Cauchy stress tensor
- $|\mathbf{g}| = 9.81$ m s^{-2} is the gravitational acceleration

Conservation of energy: not treated here.

Cauchy stress tensor

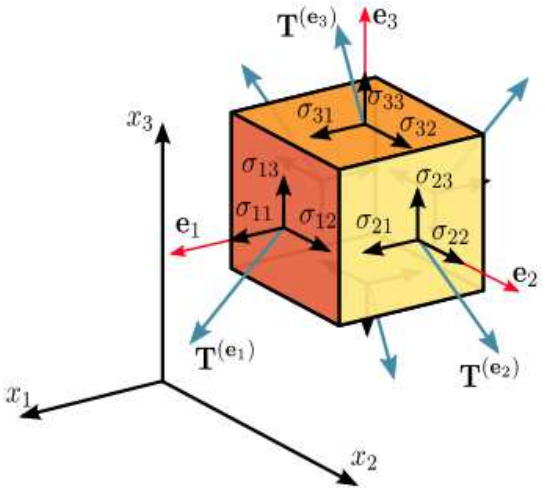

Field equations

Simplified momentum balance:

- the acceleration term (left hand side of 3; Froude number $F_r = U/\sqrt{gh} \ll 1$) = neglected;
- Coriolis force = neglected

$$\nabla \cdot \boldsymbol{\sigma} + \rho_i \mathbf{g} = 0 \tag{4}$$

- ρ_i = 910 kg m^{-3} is the density of ice.

The conservation of angular momentum ensures that the Cauchy tensor is symmetric, i.e.

$$\boldsymbol{\sigma} - \boldsymbol{\sigma}^T = 0$$

where $\boldsymbol{\sigma}^T$ is the transpose of $\boldsymbol{\sigma}$.

Consititutive equations

- A constitutive equation relates stress to strain
- Glacier ice: polycristalline fluid with a stress-dependent viscosity
- Glen's flow law: non-linear relationship between stress and deformation

$$\dot{\varepsilon} = A\sigma_e^{n-1}\boldsymbol{\tau} \tag{5}$$

where $\boldsymbol{\tau}$ is the deviatoric stress tensor, which are those stresses remaining once the hydrostatic stresses $p\mathbf{I}$ are removed from $\boldsymbol{\sigma}$,

$$\boldsymbol{\tau} = \boldsymbol{\sigma} + p\mathbf{I} \tag{6}$$

where

$$p = -\frac{1}{3}\mathrm{tr}\boldsymbol{\sigma} \tag{7}$$

- p is the isotropic pressure;
- σ_e is the effective stress (second invariant of the stress tensor $\sigma_e^2 = \frac{1}{2}\sum \tau_{ij}\tau_{ji}$).

Constitutive equation

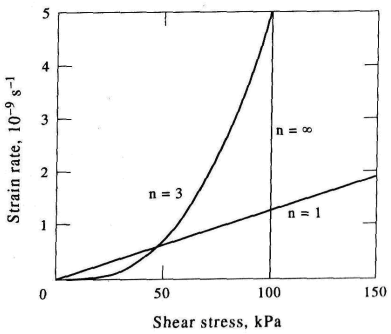

A constitutive relation links stress to strain (deformation)

$$\boldsymbol{\tau} = 2\eta\dot{\boldsymbol{\varepsilon}} \tag{8}$$

where η is the effective viscosity and $\dot{\varepsilon}$ the effective strain rate (second invariant of the strain rate tensor)

Glen's flow law:

$$\eta = \frac{1}{2}A^{-1/n}\dot{\varepsilon}_e^{(1-n)/n} \tag{9}$$

Strain rates

$\dot{\varepsilon}_e$ is the effective strain rate (second invariant of $\dot{\boldsymbol{\varepsilon}}$):

$$2\dot{\varepsilon}_e^2 = \dot{\varepsilon}_{xx}^2 + \dot{\varepsilon}_{yy}^2 + \dot{\varepsilon}_{zz}^2 + 2\left(\dot{\varepsilon}_{xy}^2 + \dot{\varepsilon}_{xz}^2 + \dot{\varepsilon}_{yz}^2\right)$$

The components of $\dot{\boldsymbol{\varepsilon}}$ are defined as,

$$\dot{\varepsilon}_{ij} = \frac{1}{2}\left(\frac{\partial v_i}{\partial x_j} + \frac{\partial v_j}{\partial x_i}\right) \tag{10}$$

Substituting (8) into the simplified momentum balance equation (4), results in the equation of motion,

$$-\nabla p + \nabla \cdot \left[\eta\left(\nabla \mathbf{v} + (\nabla \mathbf{v})^T\right)\right] + \rho_i \mathbf{g} = 0 \tag{11}$$

Boundary conditions

At the upper surface of the ice sheet s a stress free conditions is assumed,

$$\boldsymbol{\sigma} \cdot \mathbf{n} = 0 \tag{12}$$

where $\mathbf{n}$ is the outward-pointing unit normal vector. At the base of the ice sheet, basal traction $\boldsymbol{\tau}_b$ is the tangential component of the stress vector at the bed $\boldsymbol{\sigma}|_{z=b}$,

$$\boldsymbol{\tau}_b = \begin{cases} -C|\mathbf{v}_b|^{m-1}\mathbf{v}_b & h\frac{\rho_i}{\rho_w} > -b \\ 0 & \text{otherwise} \end{cases} \tag{13}$$

where h is the ice thickness, b the bedrock elevation, and ρ_w the density of seawater. Basal traction is zero when the ice sheet starts to get afloat and forms an ice shelf. $\boldsymbol{\tau}_b$ follows a sliding law where the ice grounded on bedrock, with C and m being parameters of the chosen law. Finally,

$$\mathbf{v}.\mathbf{n} = 0 \tag{14}$$

If the ice is in contact with water (such as an ice shelf), then water pressure is applied to the ice-water interface,

$$\boldsymbol{\sigma}.\mathbf{n} = \rho_w g z \mathbf{n} \tag{15}$$

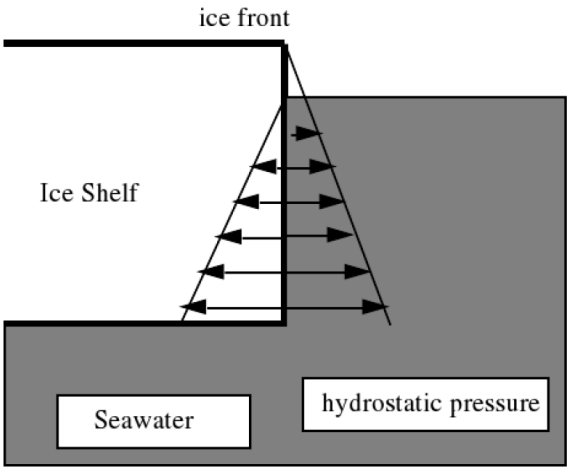

Approximations to the Stokes equations (FS)

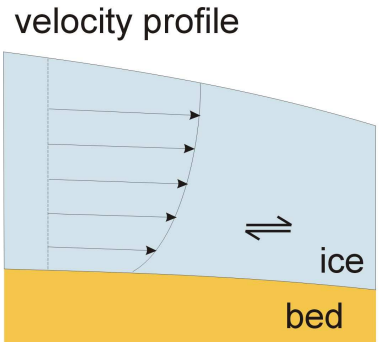

Ice sheet: vertical shearing

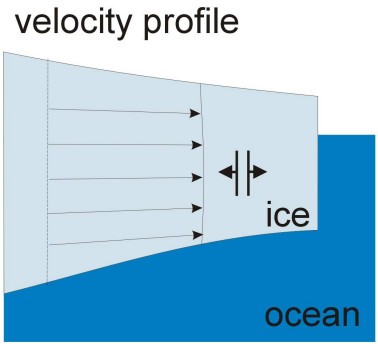

Ice shelf: longitudinal stretching

Approximations to the Stokes equations (FS)

Full stress tensor

$$\frac{\partial \tau_{xx}}{\partial x} + \frac{\partial \tau_{xy}}{\partial y} + \frac{\partial \tau_{xz}}{\partial z} = \frac{\partial p}{\partial x} \tag{16}$$

$$\frac{\partial \tau_{xy}}{\partial x} + \frac{\partial \tau_{yy}}{\partial y} + \frac{\partial \tau_{yz}}{\partial z} = \frac{\partial p}{\partial y} \tag{17}$$

$$\frac{\partial \tau_{xz}}{\partial x} + \frac{\partial \tau_{yz}}{\partial y} + \frac{\partial \tau_{zz}}{\partial z} = \frac{\partial p}{\partial z} + \rho_i g \tag{18}$$

- Blatter–Pattyn models (LMLa)
- Shallow shelf approximation (SSA or L1L1)
- Shallow-ice approximation (SIA or S)
- Hybrid models
  - Schoof–Hindmarsh (L1L2)
  - Bueler (L1L1*)

Blatter–Pattyn models (LMLa)

Simplifies the full-Stokes equations by making two assumptions: (i) a **hydrostatic assumption** is made in the vertical direction, i.e. shear stress gradients are small compared to the vertical normal stress gradients,

$$\frac{\partial \tau_{xz}}{\partial x}, \frac{\partial \tau_{yz}}{\partial y} \ll \frac{\partial \tau_{zz}}{\partial z} \tag{19}$$

This leads to reducing the vertical momentum balance (18) to

$$\frac{\partial \tau_{zz}}{\partial z} = \frac{\partial p}{\partial z} + \rho_i g \tag{20}$$

This can be integrated to give an explicit expression for p,

$$p = \tau_{zz}(z) + \rho_i g(s - z) \tag{21}$$

which means that the vertical normal stresses are balanced by the hydrostatic pressure.

This can be used to eliminate pressure from the momentum balance equations:

$$\frac{\partial \tau_{xx}}{\partial x} - \frac{\partial \tau_{zz}}{\partial x} + \frac{\partial \tau_{xy}}{\partial y} + \frac{\partial \tau_{xz}}{\partial z} = \rho_i g \frac{\partial s}{\partial x} \tag{22}$$

$$\frac{\partial \tau_{yx}}{\partial x} - \frac{\partial \tau_{zz}}{\partial y} + \frac{\partial \tau_{yy}}{\partial y} + \frac{\partial \tau_{yz}}{\partial z} = \rho_i g \frac{\partial s}{\partial y} \tag{23}$$

Due to the incompressibility condition, $\tau_{zz} = -\tau_{xx} - \tau_{yy}$, terms including the vertical normal deviatoric stress τ_{zz} can be written in terms of horizontal normal deviatoric stresses,

$$2\frac{\partial \tau_{xx}}{\partial x} + \frac{\partial \tau_{yy}}{\partial x} + \frac{\partial \tau_{xy}}{\partial y} + \frac{\partial \tau_{xz}}{\partial z} = \rho_i g \frac{\partial s}{\partial x} \tag{24}$$

$$2\frac{\partial \tau_{yy}}{\partial y} + \frac{\partial \tau_{xx}}{\partial y} + \frac{\partial \tau_{xy}}{\partial x} + \frac{\partial \tau_{yz}}{\partial z} = \rho_i g \frac{\partial s}{\partial y} \tag{25}$$

These can be written in terms of velocity components (u, v, w) by using the constitutive equation for the stress-strain relationship (8) and (10),

$$\begin{aligned}
\frac{\partial}{\partial x}\left(4\eta\frac{\partial u}{\partial x}+2\eta\frac{\partial v}{\partial y}\right)+\frac{\partial}{\partial y}\left(\eta\frac{\partial u}{\partial y}+\eta\frac{\partial v}{\partial x}\right)+\frac{\partial}{\partial z}\left(\eta\frac{\partial u}{\partial z}+\eta\frac{\partial w}{\partial x}\right) &= \rho_i g\frac{\partial s}{\partial x}\\
\frac{\partial}{\partial y}\left(4\eta\frac{\partial v}{\partial y}+2\eta\frac{\partial u}{\partial x}\right)+\frac{\partial}{\partial x}\left(\eta\frac{\partial v}{\partial x}+\eta\frac{\partial u}{\partial y}\right)+\frac{\partial}{\partial z}\left(\eta\frac{\partial v}{\partial z}+\eta\frac{\partial w}{\partial y}\right) &= \rho_i g\frac{\partial s}{\partial y}
\end{aligned}$$

Further terms can be eliminated based on the aspect ratios of ice sheets,

$$\frac{\frac{\partial w}{\partial x}}{\frac{\partial u}{\partial z}},\ \frac{\frac{\partial w}{\partial y}}{\frac{\partial v}{\partial z}} \sim \frac{\frac{0.1\ \mathrm{m\ a^{-1}}}{10^6\ \mathrm{m}}}{\frac{100\ \mathrm{m\ a^{-1}}}{1000\ \mathrm{m}}} = 10^{-6} \tag{26}$$

$$\begin{aligned}
\frac{\partial}{\partial x}\left(4\eta\frac{\partial u}{\partial x}+2\eta\frac{\partial v}{\partial y}\right)+\frac{\partial}{\partial y}\left(\eta\frac{\partial u}{\partial y}+\eta\frac{\partial v}{\partial x}\right)+\frac{\partial}{\partial z}\left(\eta\frac{\partial u}{\partial z}\right) &= \rho_i g\frac{\partial s}{\partial x}\\
\frac{\partial}{\partial y}\left(4\eta\frac{\partial v}{\partial y}+2\eta\frac{\partial u}{\partial x}\right)+\frac{\partial}{\partial x}\left(\eta\frac{\partial v}{\partial x}+\eta\frac{\partial u}{\partial y}\right)+\frac{\partial}{\partial z}\left(\eta\frac{\partial v}{\partial z}\right) &= \rho_i g\frac{\partial s}{\partial y}
\end{aligned}$$

Blatter–Pattyn models (LMLa)

Main assumption: hydrostatic approximation in the vertical

What is right?

- Different from Full Stokes: excludes resistive stresses (ability for ice to resist motion by moving up instead of out)
- Different from SSA: Incorporates vertical shearing
- Different from SIA: incorporate longitudinal stress (ability for ice to “push” downstream ice)

What is wrong?

- More complex to solve than SSA or SIA
- Much slower to compute than SSA or SIA
- Hydrostatic approximation may not be valid at grounding lines

Shallow shelf approximations (SSA or L1L1)

SSA neglects vertical shear stresses above the ice base. In ice streams and ice shelves, the basal sliding is greater than the vertical shear and membrane stresses dominate the stress balance:

$$\frac{\partial \tau_{xx}}{\partial x} + \frac{\partial \tau_{xy}}{\partial y} = \frac{\partial p}{\partial x} \tag{27}$$

$$\frac{\partial \tau_{xy}}{\partial x} + \frac{\partial \tau_{yy}}{\partial y} = \frac{\partial p}{\partial y} \tag{28}$$

$$\frac{\partial \tau_{zz}}{\partial z} = \frac{\partial p}{\partial z} + \rho_i g \tag{29}$$

This assumption automatically reduces the model to the hydrostatic approximation as seen with the Blatter-Pattyn models,

$$2\frac{\partial \tau_{xx}}{\partial x} + \frac{\partial \tau_{yy}}{\partial x} + \frac{\partial \tau_{xy}}{\partial y} = \rho_i g \frac{\partial s}{\partial x} \tag{30}$$

$$2\frac{\partial \tau_{yy}}{\partial y} + \frac{\partial \tau_{xx}}{\partial y} + \frac{\partial \tau_{xy}}{\partial x} = \rho_i g \frac{\partial s}{\partial y} \tag{31}$$

This pair of equations can be integrated in the vertical,

$$\frac{\partial}{\partial x}\left(2\eta h\left(2\frac{\partial u}{\partial x}+\eta\frac{\partial v}{\partial y}\right)\right)+\frac{\partial}{\partial y}\left(\eta h\left(\frac{\partial u}{\partial y}+\eta\frac{\partial v}{\partial x}\right)\right) = \rho_i g h\frac{\partial s}{\partial x} \quad (32)$$

$$\frac{\partial}{\partial y}\left(2\eta h\left(2\frac{\partial v}{\partial y}+\eta\frac{\partial u}{\partial x}\right)\right)+\frac{\partial}{\partial x}\left(\eta h\left(\frac{\partial v}{\partial x}+\eta\frac{\partial u}{\partial y}\right)\right) = \rho_i g h\frac{\partial s}{\partial y} \quad (33)$$

SSA reduces the problem to a two-dimensional elliptic one. With the addition of a basal traction term, they also are capable of modelling ice streams,

$$\frac{\partial}{\partial x}\left(2\eta h\left(2\frac{\partial u}{\partial x}+\eta\frac{\partial v}{\partial y}\right)\right)+\frac{\partial}{\partial y}\left(\eta h\left(\frac{\partial u}{\partial y}+\eta\frac{\partial v}{\partial x}\right)\right)-\beta^2 u = \rho_i g h\frac{\partial s}{\partial x}$$

$$\frac{\partial}{\partial y}\left(2\eta h\left(2\frac{\partial v}{\partial y}+\eta\frac{\partial u}{\partial x}\right)\right)+\frac{\partial}{\partial x}\left(\eta h\left(\frac{\partial v}{\partial x}+\eta\frac{\partial u}{\partial y}\right)\right)-\beta^2 v = \rho_i g h\frac{\partial s}{\partial y}$$

where $\tau_b = \beta^2\mathbf{v}$ is the basal drag and β^2 a friction parameter.

Effective viscosity

$$2\dot{\varepsilon}_e^2 = \dot{\varepsilon}_{xx}^2 + \dot{\varepsilon}_{yy}^2 + \dot{\varepsilon}_{zz}^2 + 2\left(\dot{\varepsilon}_{xy}^2 + \dot{\varepsilon}_{xz}^2 + \dot{\varepsilon}_{yz}^2\right)$$

Neglecting vertical shear strain components

$$\begin{aligned}
\eta &= \frac{1}{2}A^{-1/n}\dot{\varepsilon}_e^{\frac{1-n}{n}} \\
&= \frac{1}{2}A^{-1/n}\left(\frac{1}{2}\left(\dot{\varepsilon}_{xx}^2 + \dot{\varepsilon}_{yy}^2 + \dot{\varepsilon}_{zz}^2\right) + \dot{\varepsilon}_{xy}^2\right)^{\frac{1-n}{2n}} \\
&= \frac{1}{2}A^{-1/n}\left(\dot{\varepsilon}_{xy}^2 + \dot{\varepsilon}_{xx}\dot{\varepsilon}_{yy} + \dot{\varepsilon}_{xx}^2 + \dot{\varepsilon}_{yy}^2\right)^{\frac{1-n}{2n}} \\
&= \frac{1}{2}A^{-1/n}\left(\frac{1}{4}\left(\frac{\partial u}{\partial y} + \frac{\partial v}{\partial x}\right)^2 + \frac{\partial u}{\partial x}\frac{\partial v}{\partial y} + \left(\frac{\partial u}{\partial x}\right)^2 + \left(\frac{\partial v}{\partial y}\right)^2\right)^{\frac{1-n}{2n}}
\end{aligned}$$

Shallow shelf approximations (SSA or L1L1)

What is right?

- Vertically averaged model
- Model response of ice to non-local, non-gravitational effects
- Upstream ice can “push” downstream ice

What is wrong?

- Valid for ice shelves and low-drag ice streams
- Because vertically integrated, will predict no motion over frozen bed
- Does not holistically model entire system
- Effort needed to integrate with SIA model

Shallow ice approximation (SIA or S)

Only the vertical gradients of the vertical shear stresses are of interest,

$$\frac{\partial \tau_{xz}}{\partial z} = \frac{\partial p}{\partial x} \tag{34}$$

$$\frac{\partial \tau_{yz}}{\partial z} = \frac{\partial p}{\partial y} \tag{35}$$

$$0 = \frac{\partial p}{\partial z} + \rho_i g \tag{36}$$

Integrating the momentum balance equations:

$$\int_z^s \frac{\partial \tau_{xz}}{\partial z} \mathrm{d}z = \int_z^s \frac{\partial p}{\partial x} \mathrm{d}z \tag{37}$$

$$\int_z^s \frac{\partial \tau_{yz}}{\partial z} \mathrm{d}z = \int_z^s \frac{\partial p}{\partial y} \mathrm{d}z \tag{38}$$

$$p(s) - p(z) = \rho_i g (s - z) \tag{39}$$

with the stress-free condition at the surface this leads to

$$\tau_{xz}(z) = -\rho_i g(s-z)\frac{\partial s}{\partial x} \tag{40}$$

$$\tau_{yz}(z) = -\rho_i g(s-z)\frac{\partial s}{\partial y} \tag{41}$$

These equations show that the SIA stress field can be fully determined if the local geometry is known (surface elevation, ice thickness and slope). The effective stress is reduced to

$$\sigma_e = \sqrt{\tau_{xz}^2 + \tau_{yz}^2} \tag{42}$$

which with (40) and (41) leads to

$$\frac{\partial u}{\partial z} = -2A\left[\rho_i g(s-z)\right]^n |\nabla s|^{n-1} \frac{\partial s}{\partial x} \tag{43}$$

$$\frac{\partial v}{\partial z} = -2A\left[\rho_i g(s-z)\right]^n |\nabla s|^{n-1} \frac{\partial s}{\partial y} \tag{44}$$

The horizontal velocity field is determined by integrating (43) and (44) from the base of the ice sheet b to a height z:

$$u(z) - u(b) = -2A(\rho_i g)^n |\nabla s|^{n-1} \frac{\partial s}{\partial x} \int_b^z (s-z)^n \mathrm{d}z \tag{45}$$

$$v(z) - v(b) = -2A(\rho_i g)^n |\nabla s|^{n-1} \frac{\partial s}{\partial y} \int_b^z (s-z)^n \mathrm{d}z \tag{46}$$

which leads to

$$u(z) - u(b) = \frac{2A}{n+1}(\rho_i g)^n |\nabla s|^{n-1} \frac{\partial s}{\partial x} \left[(s-z)^{n+1} - h^{n+1}\right] \tag{47}$$

$$v(z) - v(b) = \frac{2A}{n+1}(\rho_i g)^n |\nabla s|^{n-1} \frac{\partial s}{\partial y} \left[(s-z)^{n+1} - h^{n+1}\right] \tag{48}$$

The vertical mean horizontal velocity is obtained by integrating (47) and (48) once more from the base of the ice mass to the surface, divided over the ice thickness h, which leads to

$$\overline{u} - u(b) = -\frac{2A}{n+2} (\rho_i g)^n |\nabla s|^{n-1} \frac{\partial s}{\partial x} h^{n+1} \quad (49)$$

$$\overline{v} - v(b) = -\frac{2A}{n+2} (\rho_i g)^n |\nabla s|^{n-1} \frac{\partial s}{\partial y} h^{n+1} \quad (50)$$

This can also be written as,

$$\overline{u} - u(b) = \frac{2A}{n+2} h |\tau_d|^{n-1} \tau_{dx} \quad (51)$$

$$\overline{v} - v(b) = \frac{2A}{n+2} h |\tau_d|^{n-1} \tau_{dy} \quad (52)$$

where τ_{dx} is the driving stress in the x direction defined by $\tau_{dx} = -\rho g h \frac{\partial s}{\partial x}$ (idem for τ_{dy}).

Shallow ice approximation (SIA or S)

What is right?

- Simplest version of the Stokes equations
- What really matters: vertical deformation in response to gravity
- Ice physics is purely local
- The shallow ice approximation is valid for ice masses experiencing little sliding and with aspect ratio $H \ll L$, where H is the thickness scale and L the length scale

What is wrong?

- Not valid for key areas in ice sheets (e.g. grounding lines)
- Not useful for ice shelves at all
- Not able to produce short time scale effects

Schoof–Hindmarsh: L1L2

- Implemented in, e.g., the BISICLES model.
- Compared to the SSA model, the second invariant of the deviatoric stress tensor takes also into account the vertical shear stresses, which are then approximated by the SIA model.
- The deviatoric stress tensor $\boldsymbol{\tau}$ is broken down as the sum of two matrices, one for the vertical shear stresses ϕ, and one for the other stresses ψ,

$$\begin{pmatrix} \tau_{xx} & \tau_{xy} & \tau_{xz} \\ \tau_{xy} & \tau_{yy} & \tau_{yz} \\ \tau_{xz} & \tau_{yz} & \tau_{zz} \end{pmatrix} = \begin{pmatrix} \tau_{xx} & \tau_{xy} & 0 \\ \tau_{xy} & \tau_{yy} & 0 \\ 0 & 0 & \tau_{zz} \end{pmatrix} + \begin{pmatrix} 0 & 0 & \tau_{xz} \\ 0 & 0 & \tau_{yz} \\ \tau_{xz} & \tau_{yz} & 0 \end{pmatrix} = \psi + \phi \tag{53}$$

where $\tau_{xz} = -\rho_i g(s-z)\frac{\partial s}{\partial x}$ and $\tau_{yz} = -\rho_i g(s-z)\frac{\partial s}{\partial y}$, both determined from SIA.

Considering the vertical shear stresses in the effective viscosity, but not in the stress tensor, Glen's flow law then becomes

$$\dot{\varepsilon}_e = A\left(\psi_e^2 + \phi_e^2\right)^{(n-1)/2}\boldsymbol{\psi} \tag{54}$$

where ψ_e is the second invariant of $\boldsymbol{\psi}$, and ϕ_e is the second invariant of $\boldsymbol{\psi}$, given by the SIA as

$$\phi_e^2 = (\rho_i g(s-z))^2\left[\left(\frac{\partial s}{\partial x}\right)^2 + \left(\frac{\partial s}{\partial y}\right)^2\right] \tag{55}$$

Assuming the inverse flow law as $\boldsymbol{\psi} = 2\eta\dot{\varepsilon}$, we have $\psi_e^2 = 4\eta^2\dot{\varepsilon}_e^2$, which, combined with (54) becomes,

$$\dot{\varepsilon}_e = A\left(4\eta^2\dot{\varepsilon}_e^2 + \phi_e^2\right)^{(n-1)/2}\boldsymbol{\psi} \tag{56}$$

In combination with the inverse flow law, this results in,

$$2\eta A\left(4\eta^2\dot{\varepsilon}_e^2 + \phi_e^2\right) = 1 \tag{57}$$

Bueler: L1L1*

This approximation consists of employing the SSA (**v**) as a sliding law in an SIA (**u**) model. We compute the combined horizontal velocity $\mathbf{U} = (U_x, U_y)$ by

$$\mathbf{U} = f(|\mathbf{v}|)\,\mathbf{u} + (1 - f(|\mathbf{v}|))\,\mathbf{v} \tag{58}$$

where $|\mathbf{v}|^2 = v_x^2 + v_y^2$ and

$$f(|\mathbf{v}|) = 1 - \arctan\left(\frac{|\mathbf{v}|^2}{100^2}\right) \tag{59}$$

The weighting function f has values between zero and one. While this function guarantees a smooth combination between both SSA and SIA velocities, several authors simply combine both fields by addition, i.e. $\mathbf{U} = \mathbf{u} + \mathbf{v}$.

Hybrid models

What is right?

- Combines SSA with SIA for internal ice deformation
- Fast computation
- Behaviour similar to HOM

What is wrong?

- Variable ways to combine both shearing and stretching terms
- Combination not always implies effective stresses to incorporate both shearing and stretching terms
- Hydrostatic approximation may not be valid at grounding lines

Ice-sheet evolution

Mass conservation implies that

$$\frac{\partial u}{\partial x} + \frac{\partial v}{\partial y} + \frac{\partial w}{\partial z} = 0 \tag{60}$$

from which it follows that

$$w(s) - w(b) = -\int_b^s \nabla \cdot \mathbf{v}_H(z) \mathrm{d}z \tag{61}$$

where $\mathbf{v}_H$ are the components of the horizontal velocity (u, v). At the upper and lower surfaces, respectively, kinematic boundary conditions apply, i.e.,

$$w(b) = \frac{\partial b}{\partial t} + \mathbf{v}_H(b) \cdot \nabla b - \dot{a}_b \tag{62}$$

$$w(s) = \frac{\partial s}{\partial t} + \mathbf{v}_H(s) \cdot \nabla s - \dot{a}_s \tag{63}$$

where $\dot{a}_s$ and $\dot{a}_b$ are the surface and basal mass balance, respectively.

Ice-sheet evolution

Using Leibniz integration rule, we obtain

$$w(s) - w(b) = -\nabla \cdot \int_b^s \mathbf{v}_H(z)\mathrm{d}z + \mathbf{v}_H(s) \cdot \nabla s - \mathbf{v}_H(b) \cdot \nabla b \quad (64)$$

$$= -\nabla \cdot (\overline{\mathbf{v}}_H h) + \mathbf{v}_H(s) \cdot \nabla s - \mathbf{v}_H(b) \cdot \nabla b \quad (65)$$

In combination with the kinematic boundary conditions, this leads to

$$\frac{\partial h}{\partial t} = -\nabla \cdot (\overline{\mathbf{v}}_H h) + \dot{a}_s - \dot{a}_b \quad (66)$$

This is the main equation to solve, which is documented in the next section.

Applicability of approximations

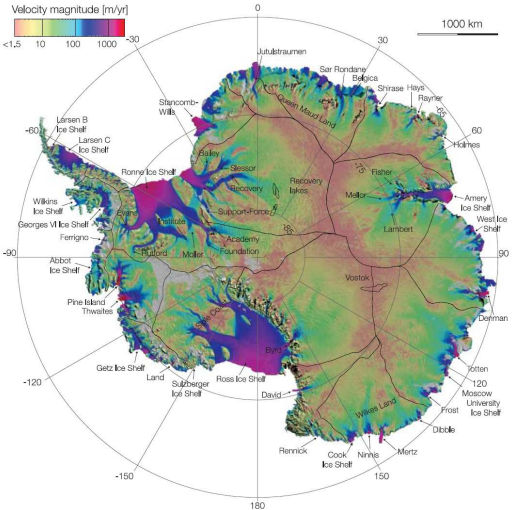

Antarctic ice velocity (Rignot et al., 2011)

Ice divides: Raymond effect

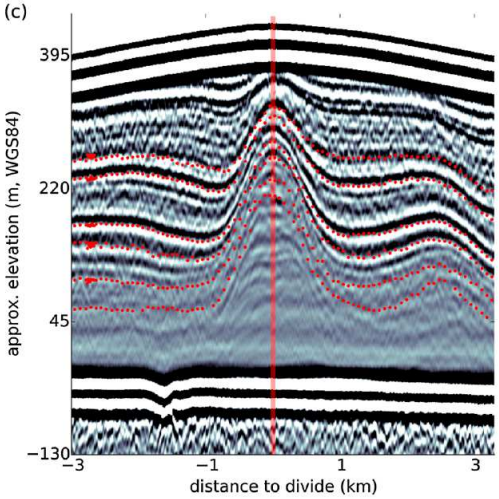

Radargram of isochrone stratigraphy across the Derwael ice rise (East Antarctica; Drews et al., 2015).

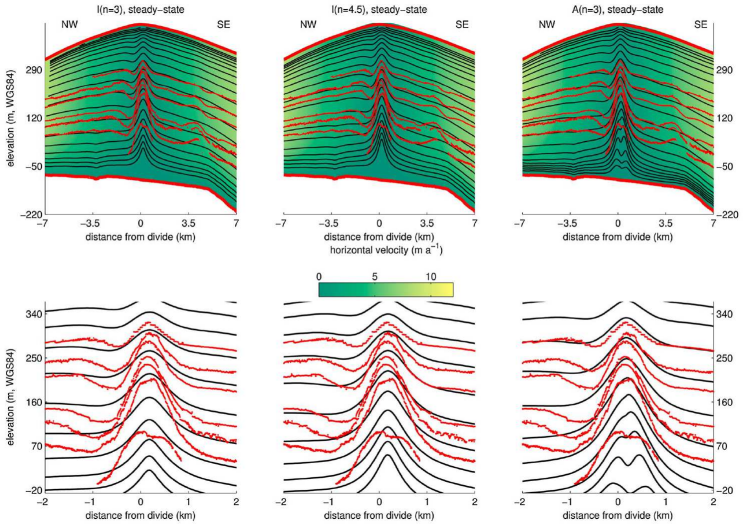

Simulated isochrones near the Derwael ice rise ice divide with a FS model (Elmer/ice) for different values of the flow exponent *n* in Glen's flow law and isotropic (I) and anisotropic (A) ice (Drews et al, 2015).

ISMIP-HOM

Ice Sheet Model Intercomparison for Higher-Order models

The basic experiment considers a parallel-sided slab of ice with a mean ice thickness h = 1000 m lying on a sloping bed with a mean slope α = 0.5°.

$$s(x, y) = -x \cdot \tan \alpha \ . \tag{67}$$

The basal topography is then given by

$$b(x, y) = s(x, y) - 1000 + 500 \sin(\omega x) \cdot \sin(\omega y) \ , \tag{68}$$

where $x \in [0, L]$ and L = 160, 80, 40, 20, 10 and 5 km.

- SIA will **always** produce same velocity field
- Distinction between full-Stokes (FS) and non-full-Stokes (NFS) models (LMLa, LTSML, L1L2 and L1L1)
- Velocities are displayed along a section $y = L/4$.

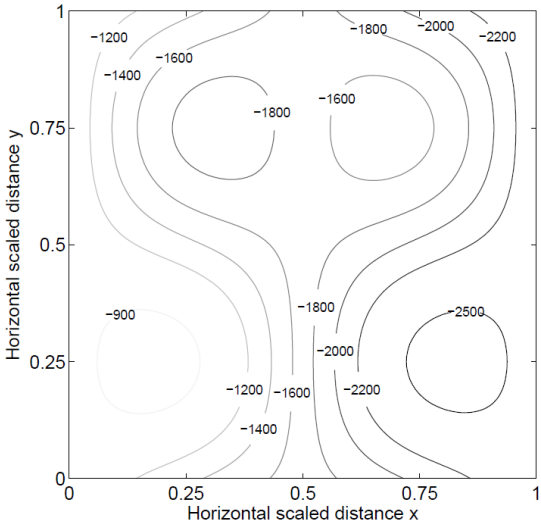

Bed elevation for the ISMIP-HOM experiment (bumpy bed).

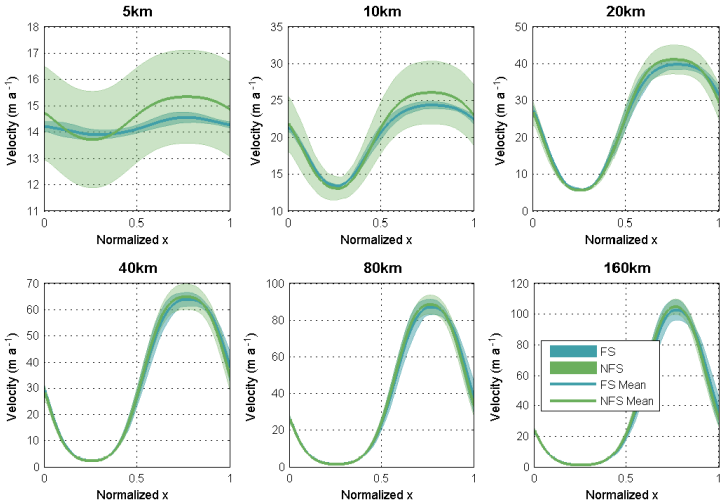

Results of the ISMIP-HOM bumpy bed experiment for different aspect ratios, i.e., different values for the length scale L for full Stokes (FS) and non-full Stokes (NFS) models (Pattyn et al., 2008).

Numerical modelling of ice sheets and ice shelves

1 Commonly used approximations in ice flow modelling

2 Numerical modelling of ice sheets (SIA)
- Numerical methods
- Explicit numerical solution for the ice-sheet equation
- Semi-implicit numerical solution of the ice-sheet equation
- Verification of SIA solutions
- Two-dimensional ice-sheet model
- EISMINT experiments
- A Greenland SIA ice sheet model

3 Numerical modelling of marine ice sheets (SSA)

Numerical methods

- Finite difference method: dividing up the model domain in regularly-spaced nodes on which the variables will be calculated.
- Replacing derivatives by discrete spatial/temporal differences or gradients, based on Taylor series,

$$H(t+\Delta t) \approx H(t) + \Delta t \frac{\partial H}{\partial t} + \frac{(\Delta t)^2}{2} \frac{\partial^2 H}{\partial t^2} + \frac{(\Delta t)^3}{6} \frac{\partial^3 H}{\partial t^3} + ... \tag{69}$$

Normally, terms higher than the second derivative are neglected, so that the time derivative is approximated by

$$\frac{\partial H}{\partial t} \approx \frac{H_{t+\Delta t} - H_t}{\Delta t} \tag{70}$$

Since time can be considered a regularly spaced vector with spacing of Δt, it is easier to use the following notation,

$$\frac{\partial H}{\partial t} \approx \frac{H_{t+1} - H_t}{\Delta t} \tag{71}$$

FTCS scheme

A similar approach is used for spatial derivatives, but contrary to the time derivative centred in space,

$$\frac{\partial H}{\partial x} \approx \frac{H_{i+1} - H_{i-1}}{2\Delta x} \tag{72}$$

$$\frac{\partial^2 H}{\partial x^2} \approx \frac{H_{i+1} - 2H_i + H_{i-1}}{(\Delta x)^2} \tag{73}$$

Such scheme is called FTCS or Forward in Time, Central in Space. The second derivative is determined by calculating local spatial gradients between consecutive grid points and taking the gradient across these points. The result is a symmetric derivative around i, involving only the immediate neighbouring grid points $i+1$ and $i-1$.

FTCS scheme

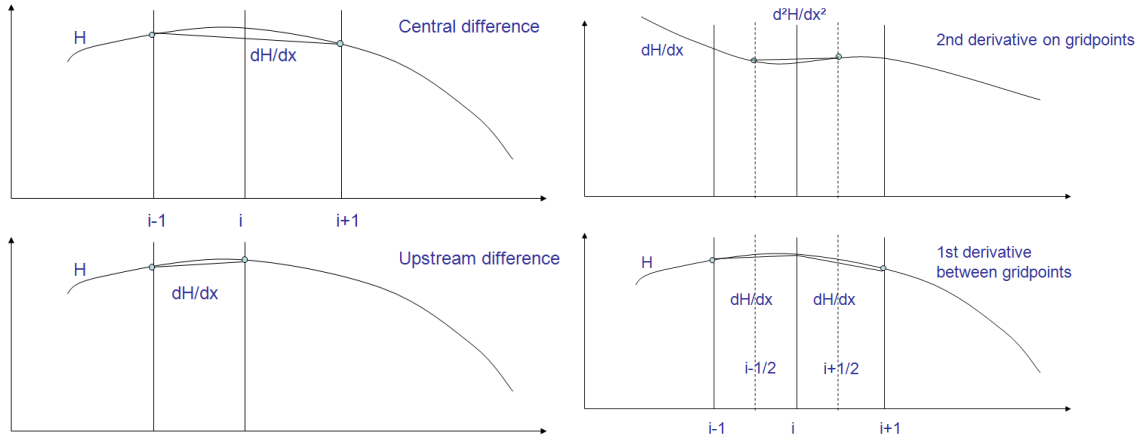

Spatial derivatives according to backward (upstream) and central differences for first (left) and second (right) order derivatives.

Explicit numerical solution for the ice-sheet equation

In order to solve the derived equations (66) and (51) numerically, we will employ the same numerical methods as illustrated above.

$$\overline{u} = -\frac{2A}{n+2}(\rho_I g)^n \left|\frac{\partial s}{\partial x}\right|^{n-1} \frac{\partial s}{\partial x} h^{n+1} \tag{74}$$

where $s = b + h$ is the surface elevation of the ice sheet. Basal melting is neglected and surface mass balance is governed by a constant accumulation rate $\dot{a}$, so that (66) transforms to,

$$\frac{\partial h}{\partial t} = -\frac{\partial(\overline{u}h)}{\partial x} + \dot{a} = -\frac{\partial q}{\partial x} + \dot{a} \tag{75}$$

Explicit numerical solution for the ice-sheet equation

Numerically, this is written as,

$$h_{i,t+1} = h_{i,t} + \left[q_{i+\frac{1}{2},t} - q_{i-\frac{1}{2},t} \right] \frac{\Delta t}{\Delta x} + \dot{a} \Delta t \tag{76}$$

where the fluxes inbetween grid points are defined as,

$$q_{i+\frac{1}{2},t} = \frac{2A}{n+2} (\rho_i g)^n \left(\frac{h_{i+1,t} + b_{i+1,t} - h_{i,t} - b_{i,t}}{\Delta x} \right)^n \left(\frac{h_{i,t} + h_{i+1,t}}{2} \right)^{n+2} \tag{77}$$

$$q_{i-\frac{1}{2},t} = \frac{2A}{n+2} (\rho_i g)^n \left(\frac{h_{i,t} + b_{i,t} - h_{i-1,t} - b_{i-1,t}}{\Delta x} \right)^n \left(\frac{h_{i,t} + h_{i-1,t}}{2} \right)^{n+2} \tag{78}$$

In reality, the continuity equation is a diffusion equation due to the dependence of q on $\partial h/\partial x$

$$\begin{aligned} \frac{\partial h}{\partial t} &= -\frac{\partial}{\partial x}(\overline{u}h) + \dot{a} \\ &= \frac{\partial}{\partial x}\left(d\frac{\partial(h+b)}{\partial x}\right) + \dot{a} \end{aligned} \tag{79}$$

where the (spatially-varying) diffusion coefficient d is defined by

$$\begin{aligned} d &= -\overline{u}h\left(\frac{\partial(h+b)}{\partial x}\right)^{-1} \\ &= -\frac{2A}{n+2}(\rho_i g)^n \left|\frac{\partial(h+b)}{\partial x}\right|^{n-1} h^{n+2} \end{aligned} \tag{80}$$

Diffusion terms (or transformed flux terms) are evaluated between the grid points

$$d_{i+\frac{1}{2},t} = \frac{2A}{n+2}(\rho_i g)^n \left| \frac{h_{i+1,t} + b_{i+1,t} - h_{i,t} - b_{i,t}}{\Delta x} \right|^{n-1} \left(\frac{h_{i,t} + h_{i+1,t}}{2} \right)^{n+2} \tag{81}$$

$$\begin{aligned} h_{i,t+1} &= h_{i,t} + \frac{\Delta t}{(\Delta x)^2} \Big[d_{i+\frac{1}{2},t}(h_{i+1,t} + b_{i+1,t} - h_{i,t} - b_{i,t}) - \\ &\quad d_{i-\frac{1}{2},t}(h_{i,t} + b_{i,t} - h_{i-1,t} - b_{i-1}) \Big] + \dot{a}\Delta t \end{aligned} \tag{82}$$

The diffusive grid is called a staggered grid, similar to the flux-equation shown before. Boundary conditions for (82) are zero ice thickness at the boundaries.

Code: initialization

```
m=51;
L=1.5e6; % length of domain (m)
h=zeros(m,1);
time_end=20000.;
dt=2.; % time step (years)
dx=L/(m-1); % grid spacing (m)
x=linspace(0,L,m)'; % horizontal distance
b=zeros(m,1); % bedrock elevation
d=zeros(m,1);

% Physical constants
A=1e-16; % Ice flow parameter
rho=910.; % Ice density
grav=9.81; % Gravitation constant
n=3; % Glen index
a=0.3; % Surface mass balance
```

Code: body

```
% time stepping
time_lapse = round(time_end/dt)+1;
h2=h;
for i=1:time_lapse
    slope=diff(b+h)/dx; % slope on staggered grid
    for j=1:m-1
        hstag=(h(j+1)+h(j))/2.; % ice thickness on staggered grid
        d(j)=2./(n+2.)*A*hstag^2*slope(j)^2*(rho* ...
            grav*hstag)^n;
    end
    for j=2:m-1
        h2(j)=h(j)+(d(j)*slope(j)-d(j-1)*slope(j-1))*dt/dx+a*dt;
    end
    h=h2;
end %% end of time stepping
```

Code: body vectorized

```
% time stepping
time_lapse = round(time_end/dt)+1;
h2=h;
for i=1:time_lapse
    slope=diff(b+h)/dx; % slope on staggered grid
    slope(m)=0;
    hstag=(circshift(h,[-1 0])+h)/2;
    dif=2/(n+2.)*A*(hstag.^2).*(slope.^2).*(rho_ice*grav*hstag).^n;
    h2=h+(dif.*slope-circshift(dif,[1 0]).*circshift(slope,[1 0]))* ...
        dt/gridx+a*dt;
    h2(1)=0;
    h2(m)=0;
    h=h2;
end %% end of time stepping
```

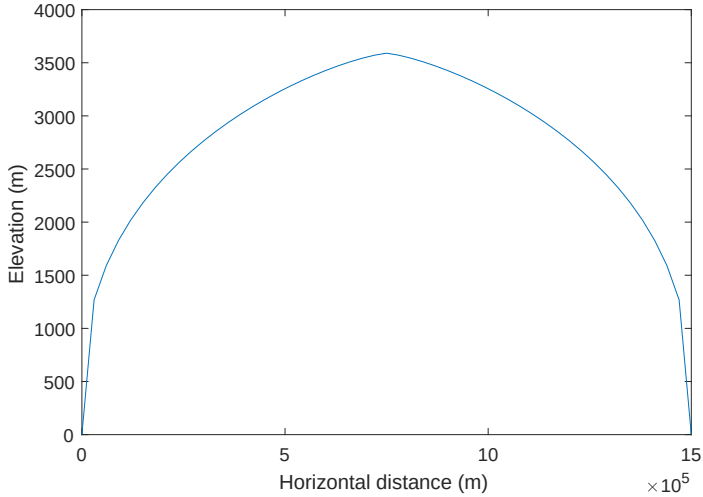

Evolution of an ice sheet on a flat bedrock based on the solution of (82)

Semi-implicit solution of the ice-sheet equation

Greater numerical stability can be obtained by invoking a Crank-Nicholson scheme:

$$\frac{H_{t+1} - H_t}{\Delta t} = (1-\omega)\frac{\partial H}{\partial t}|_t + \omega \frac{\partial H}{\partial t}|_{t+1} \tag{83}$$

with ω=0 (explicit) or ω=1 (implicit). For ω=1, this leads to:

$$\begin{aligned} h_{i,t+1} &= h_{i,t} + \frac{\Delta t}{(\Delta x)^2}\Big[d_{i+\frac{1}{2},t}(h_{i+1,t+1} + b_{i+1,t} - h_{i,t+1} - b_{i,t}) - \\ &\quad d_{i-\frac{1}{2},t}(h_{i,t+1} + b_{i,t} - h_{i-1,t+1} - b_{i-1,t})\Big] + \dot{a}\Delta t \end{aligned} \tag{84}$$

$$\begin{aligned} &h_{i,t+1} - \frac{\Delta t}{(\Delta x)^2}\left[d_{i+\frac{1}{2},t}(h_{i+1,t+1} - h_{i,t+1}) - d_{i-\frac{1}{2},t}(h_{i,t+1} - h_{i-1,t+1})\right] \\ &= \frac{\Delta t}{(\Delta x)^2}\left[d_{i+\frac{1}{2},t}(b_{i+1,t} - b_{i,t}) - d_{i-\frac{1}{2},t}(b_{i,t} - b_{i-1,t})\right] + \dot{a}\Delta t \end{aligned} \tag{85}$$

We can define the following coefficients that remain a function of h:

$$\alpha_i = \frac{\Delta t}{(\Delta x)^2} d_{i-\frac{1}{2},t} \qquad \beta_i = 1 + \frac{\Delta t}{(\Delta x)^2}\left(d_{i-\frac{1}{2},t} + d_{i+\frac{1}{2},t}\right)$$
$$\gamma_i = \frac{\Delta t}{(\Delta x)^2} d_{i+\frac{1}{2},t} \qquad \delta_i = \alpha_i b_{i-1,t} - (\beta_i - 1) b_{i,t} + \gamma_i b_{i+1,t} + h_{i,t} + \dot{a}\Delta t$$

so that,

$$-\alpha_i h_{i-1,t+1} + \beta_i h_{i,t+1} - \gamma_i h_{i+1,t+1} = \delta_i \tag{86}$$

This system of equations can be written in matrix notation as follows.

$$\begin{bmatrix} \beta_1 & -\gamma_1 & 0 & 0 & \cdots & 0 & 0 & 0 \\ -\alpha_2 & \beta_2 & -\gamma_2 & 0 & \cdots & 0 & 0 & 0 \\ 0 & -\alpha_3 & \beta_3 & -\gamma_3 & \cdots & 0 & 0 & 0 \\ \vdots & \vdots & \vdots & \vdots & \ddots & \vdots & \vdots & \vdots \\ 0 & 0 & 0 & 0 & \cdots & -\alpha_{m-1} & \beta_{m-1} & -\gamma_{m-1} \\ 0 & 0 & 0 & 0 & \cdots & 0 & -\alpha_m & \beta_m \end{bmatrix} \begin{bmatrix} h_1 \\ h_2 \\ h_3 \\ \vdots \\ h_{m-1} \\ h_m \end{bmatrix} = \begin{bmatrix} \delta_1 \\ \delta_2 \\ \delta_3 \\ \vdots \\ \delta_{m-1} \\ \delta_m \end{bmatrix} \tag{87}$$

This is a tridiagonal system of equations. Consider the following two equations that hold between two adjacent grid points:

$$h_i = f_i h_{i+1} + g_i \tag{88}$$

$$h_{i-1} = f_{i-1} h_i + g_{i-1} \tag{89}$$

By definition we can derive from (86) and (89) that

$$\begin{aligned} \alpha_i h_{i-1} &= \alpha_i f_{i-1} h_i + \alpha_i g_{i-1} \\ &= \beta_i h_i - \gamma_i h_{i+1} - \delta_i \end{aligned}$$

Combining both equations then results in

$$h_i = \frac{\gamma_i}{\beta_i - \alpha_i f_{i-1}} h_{i-1} + \frac{\delta_i + \alpha_i g_{i-1}}{\beta_i - \alpha_i f_{i-1}} \tag{90}$$

where,

$$f_i = \frac{\gamma_i}{\beta_i - \alpha_i f_{i-1}}\,, \qquad g_i = \frac{\delta_i + \alpha_i g_{i-1}}{\beta_i - \alpha_i f_{i-1}}$$

For both the explicit and implicit solution, boundary conditions need to be defined, i.e., ice thickness at the first and last grid point, as well as conditions pertaining to the ice sheet velocity. For simplicity, we will consider that ice thickness at the lateral boundaries is zero (edge of the ice sheet), or $h_1 = h_m = 0$, so that $f_1 = g_1 = 0$. With $h_m = 0$, we have,

$$\begin{aligned} h_{m-1} &= f_{m-1} h_m + g_{m-1} \\ h_{m-2} &= f_{m-2} h_{m-1} + g_{m-2} \\ &\vdots \\ h_1 &= f_1 h_2 + g_1 \end{aligned}$$

```
m=51;
L=1.5e6; % length of domain (m)
h=zeros(m,1);
time_end=20000.;
dt=10.; % time step (years)
dx=L/(m-1); % grid spacing (m)
x=linspace(0,L,m)'; % horizontal distance
b=zeros(m,1); % bedrock elevation
d=zeros(m,1);
alph=zeros(m,1); bet=zeros(m,1); gamm=zeros(m,1); delta=zeros(m,1);
f=zeros(m,1); g=zeros(m,1);
% Physical constants
A=1e-16; % Ice flow parameter
rho=910.; % Ice density
grav=9.81; % Gravitation constant
n=3; % Glen index
a=0.3; % Surface mass balance
time_lapse = round(time_end/dt)+1;
dtdx=dt/dx^2;
```

```
for i=1:time_lapse
    h2=zeros(m,1); slope=diff(b+h)/dx; % slope on staggered grid
    for j=1:m-1
        hstag=(h(j+1)+h(j))/2.; % ice thickness on staggered grid
        d(j)=2./(n+2.)*A*hstag^2*slope(j)^2*(rho*grav*hstag)^n;
    end
    for j=2:m-1
        gamm(j)=d(j)*dtdx;          alph(j)=d(j-1)*dtdx;
        bet(j)=1.+gamm(j)+alph(j);
        delta(j)=h(j)+a*dt+alph(j)*b(j-1)-(bet(j)-1)*b(j) ...
            +gamm(j)*b(j+1);
    end
    for j=2:m-1
        f(j)=gamm(j)/(bet(j)-alph(j)*f(j-1));
        g(j)=(delta(j)+alph(j)*g(j-1))/(bet(j)-alph(j)*f(j-1));
    end
    for j=m-1:-1:1
        h2(j)=g(j)+f(j)*h2(j+1);
    end
    h=h2;
end %% end of time stepping
```

The Nye-Vialov analytical solution

This analytical solution is valid for an ice sheet resting on a flat bed ($b = 0$) and for a constant accumulation rate $\dot{a}$. In a steady state, it follows from mass continuity that

$$\dot{a}x = uh = -A_0 \left|\frac{\partial h}{\partial x}\right|^{n-1} \frac{\partial h}{\partial x} \tag{91}$$

where

$$A_0 = \frac{2A}{n+2} (\rho_i g)^n \tag{92}$$

The Nye-Vialov analytical solution

Integrating (91) leads to

$$\left(h^{1+2/n}\frac{\partial h}{\partial x}\right)^n = -\frac{\dot{a}}{A_0}x \tag{93}$$

$$\frac{\partial}{\partial x}\left(h^{2+2/n}\right) = -\frac{2n+2}{n}\left(\frac{\dot{a}}{A_0}\right)^{1/n} x^{1/n} \tag{94}$$

$$h^{2+2/n} = h_0^{2+2/n}\left(1-\left(\frac{|x-L|}{L}\right)^{1+1/n}\right) \tag{95}$$

where

$$h_0^{2+2/n} = \frac{2n+2}{n+1}\left(\frac{\dot{a}}{A_0}\right)^{1/n} L^{1+1/n} \tag{96}$$

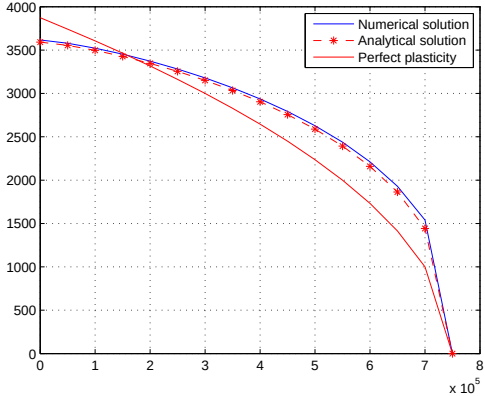

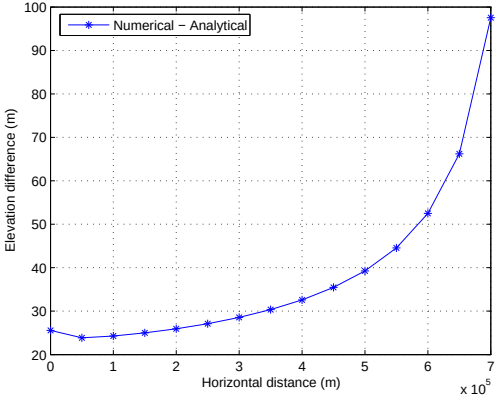

Difference between steady-state modeled (blue) and analytical (red) ice sheet profiles; differences increase towards the edge of the ice sheet domain, where ice fluxes are the highest.

$$\frac{\partial(\overline{u}h)}{\partial x} = \dot{a} \quad \text{or (by integration)} \quad \overline{u}_x h_x = \int_0^x \dot{a} dx = \dot{a}x \tag{97}$$

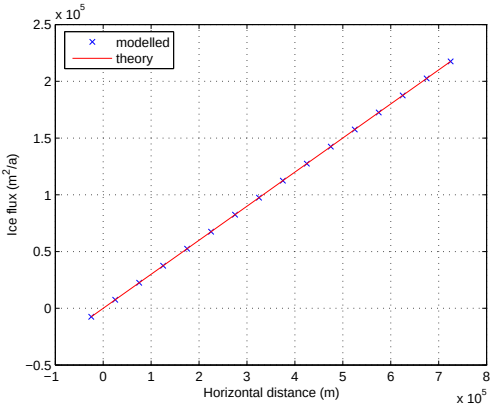

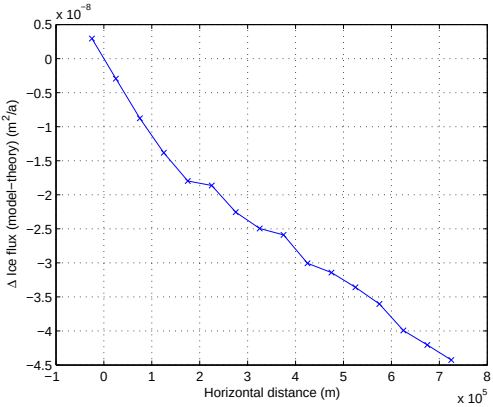

Plot of steady state ice flux versus interated accumulation rate along the flowline (left); difference between both (right).

Two-dimensional ice sheet model

- Extent the flowline model to two plane dimensions
- Boundary conditions: $H = 0$ on all lateral boundaries
- Keep constant surface mass balance

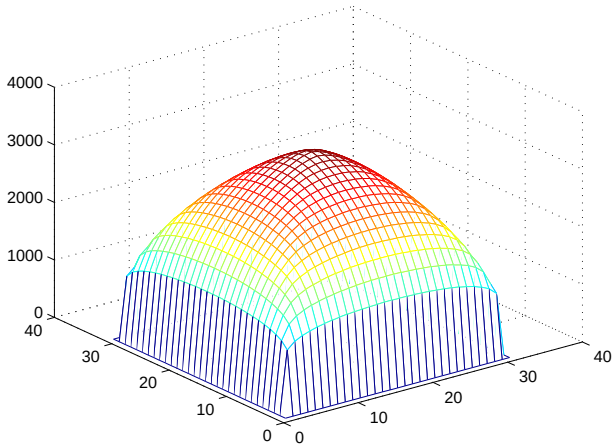

Two-dimensional ice sheet model

$$\frac{\partial h}{\partial t} = \dot{a} - \nabla \cdot \left(\frac{2(\rho g)^3 A h^5}{5} (\nabla h)^3 \right) \tag{98}$$

It will be convenient for what follows to adopt nondimensional variables. Accordingly, we set

$$\begin{aligned} h &\rightarrow Zs \\ x, y &\rightarrow Lx, Ly \end{aligned}$$

and choose scales Z and L to satisfy the following identity

$$\frac{2A(\rho g)^3 Z^8}{5L^4} = \dot{a} \tag{99}$$

For $L = 750$ km and $a = 0.3$ m/yr, the above expression gives $Z = 2756.7$m.

Implicit time-stepping with a staggered grid

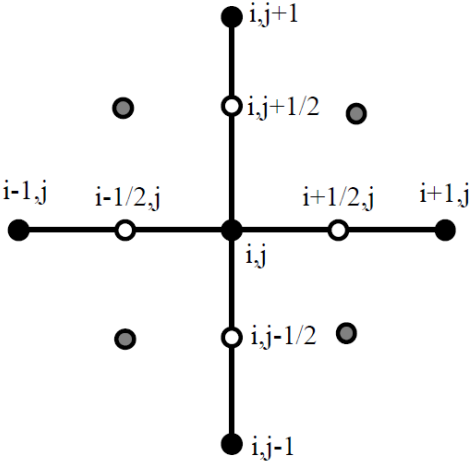

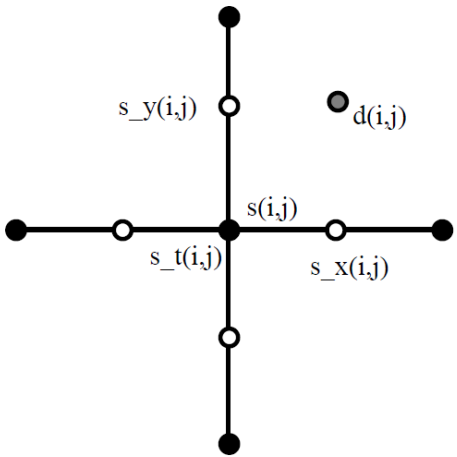

Staggered grid used for solving the ice sheet equation in a two-dimensional model.

$$
\begin{aligned}
d_{i,j}^{\ell} &= \left[\frac{1}{4}\left(s_{i,j}^{\ell}+s_{i+1,j}^{\ell}+s_{i+1,j+1}^{\ell}+s_{i,j+1}^{\ell}\right)\right]^5 \\
&\times \frac{1}{4\Delta^2}\left[\left(s_{i+1,j}^{\ell}-s_{i,j}^{\ell}+s_{i+1,j+1}^{\ell}-s_{i,j+1}^{\ell}\right)^2\right. \\
&+ \left.\left(s_{i,j+1}^{\ell}-s_{i,j}^{\ell}+s_{i+1,j+1}^{\ell}-s_{i+1,j}^{\ell}\right)^2\right]
\end{aligned}
$$

$$
\begin{aligned}
\frac{\partial}{\partial x}\left(d\frac{\partial s}{\partial x}\right)\Big|_{i,j} &= \frac{1}{2\Delta^2}\left[\left(d_{i,j}^{\ell}+d_{i,j-1}^{\ell}\right)\left(s_{i+1,j}^{\ell+1}+s_{i,j}^{\ell+1}\right)\right. \\
&- \left.\left(d_{i-1,j}^{\ell}+d_{i-1,j-1}^{\ell}\right)\left(s_{i,j}^{\ell+1}+s_{i-1,j}^{\ell+1}\right)\right] \\
\frac{\partial}{\partial y}\left(d\frac{\partial s}{\partial y}\right)\Big|_{i,j} &= \frac{1}{2\Delta^2}\left[\left(d_{i,j}^{\ell}+d_{i-1,j}^{\ell}\right)\left(s_{i,j+1}^{\ell+1}+s_{i,j}^{\ell+1}\right)\right. \\
&- \left.\left(d_{i,j-1}^{\ell}+d_{i-1,j-1}^{\ell}\right)\left(s_{i,j}^{\ell+1}+s_{i,j-1}^{\ell+1}\right)\right]
\end{aligned}
$$

$$
\begin{aligned}
s_{i,j}^{\ell+1}\left[\frac{1}{\Delta t}+\frac{1}{\Delta^2}\left(d_{i,j}^{\ell}+d_{i-1,j}^{\ell}+d_{i,j-1}^{\ell}+d_{i-1,j-1}^{\ell}\right)\right] & \\
+s_{i,j+1}^{\ell+1}\left[\frac{-1}{2\Delta^2}\left(d_{i,j}^{\ell}+d_{i-1,j}^{\ell}\right)\right] & \\
+s_{i,j-1}^{\ell+1}\left[\frac{-1}{2\Delta^2}\left(d_{i,j-1}^{\ell}+d_{i-1,j-1}^{\ell}\right)\right] & \\
s_{i+1,j}^{\ell+1}\left[\frac{-1}{2\Delta^2}\left(d_{i,j}^{\ell}+d_{i,j-1}^{\ell}\right)\right] & \\
s_{i-1,j}^{\ell+1}\left[\frac{-1}{2\Delta^2}\left(d_{i-1,j}^{\ell}+d_{i-1,j-1}^{\ell}\right)\right] & = 1+\frac{s_{i,j}^{\ell}}{\Delta t}
\end{aligned}
$$

The above equation may be conveniently expressed in matrix notation as follows:

$$\mathbf{A}s^{\ell+1}=\mathbf{R}$$

$$
\begin{aligned}
s_{i,j}^{\ell+1}\left[\frac{1}{\Delta t}+\frac{1}{\Delta^2}\left(d_{i,j}^{\ell}+d_{i-1,j}^{\ell}+d_{i,j-1}^{\ell}+d_{i-1,j-1}^{\ell}\right)\right] &\rightarrow A_{\gamma_{i,j},\gamma_{i,j}}\\
s_{i,j+1}^{\ell+1}\left[\frac{-1}{2\Delta^2}\left(d_{i,j}^{\ell}+d_{i-1,j}^{\ell}\right)\right] &\rightarrow A_{\gamma_{i,j},\gamma_{i,j+1}}\\
s_{i,j-1}^{\ell+1}\left[\frac{-1}{2\Delta^2}\left(d_{i,j-1}^{\ell}+d_{i-1,j-1}^{\ell}\right)\right] &\rightarrow A_{\gamma_{i,j},\gamma_{i,j-1}}\\
s_{i+1,j}^{\ell+1}\left[\frac{-1}{2\Delta^2}\left(d_{i,j}^{\ell}+d_{i,j-1}^{\ell}\right)\right] &\rightarrow A_{\gamma_{i,j},\gamma_{i+1,j}}\\
s_{i-1,j}^{\ell+1}\left[\frac{-1}{2\Delta^2}\left(d_{i-1,j}^{\ell}+d_{i-1,j-1}^{\ell}\right)\right] &\rightarrow A_{\gamma_{i,j},\gamma_{i-1,j}}\\
1+\frac{s_{i,j}^{\ell}}{\Delta t} &\rightarrow R_{\gamma_{i,j}}
\end{aligned}
$$

$$A_{\gamma_{i,j},\gamma_{i,j}}=1 \qquad \text{for } i=1,i_{\max}\, j=1,j_{\max}$$

$$R_{\gamma_{i,j}}=0 \qquad \text{for } i=1,i_{\max}\, j=1,j_{\max}$$

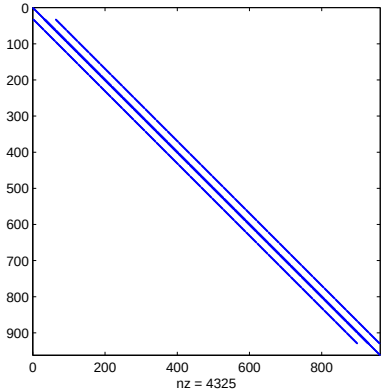

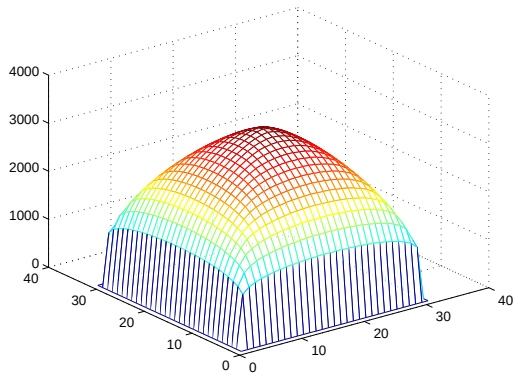

Left: Non-zero elements in the sparse matrix **A**. Right: Two-dimensional ice sheet solved using the sparse matrix solver illustrated above.

EISMINT fixed margin experiment

- The EISMINT-I benchmark is the first series of ice-sheet model intercomparisons aiming at benchmarking large-scale ice sheet models under idealized and controlled conditions (Huybrechts et al, 1996).
- The fixed margin experiment considers a square grid of 1500 $\times$ 1500 km with a flat bed at zero elevation, $\Delta = 50$ km (31 by 31 grid points)
- Starting from zero ice thickness, the model is forced with $\dot{a}$= 0.3 m a^{-1}.
- $A = 10^{16}$ Pa^{-n} a^{-1}
- $H = 0$ at the grid boundaries

Exp	Variable	Benchmark	SIA model
FM	h_{summit}	3419.90$\pm$1.70	3421.82
	q_{midpoint}	789.95$\pm$1.83	790.43

EISMINT fixed margin experiment

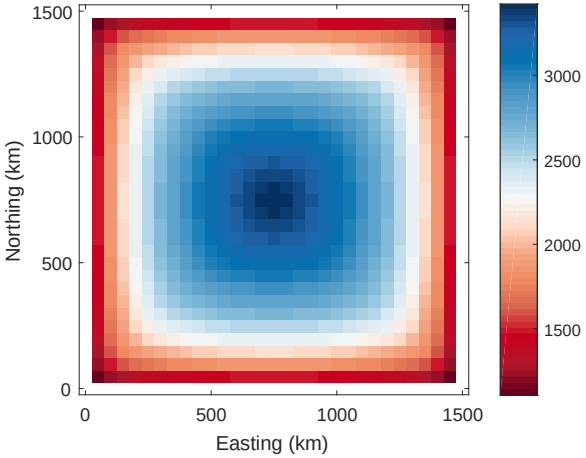

Modelled ice thickness according to the EISMINT-FM experiment.

EISMINT moving margin experiment

- The moving-margin experiment includes ice ablation, hence the presence of an equilibrium line on the ice sheet.
- $\dot{a} = \min\{0.5, s(R_{\text{el}} - d_{\text{summit}})\}$, where d_{summit} is the radial distance from the centre (in km), and s and R_{el} are 10^{-2} m a^{-1} km^{-1} and 450 km, respectively
- The steady-state ice sheet according to this experiment does not reach the edge of the domain, but is circular in shape.

Exp	Variable	Benchmark	SIA model
MM	h_{summit}	2997.5±7.4	2986.41
	q_{midpoint}	999.24±17.91	994.49

EISMINT moving margin experiments

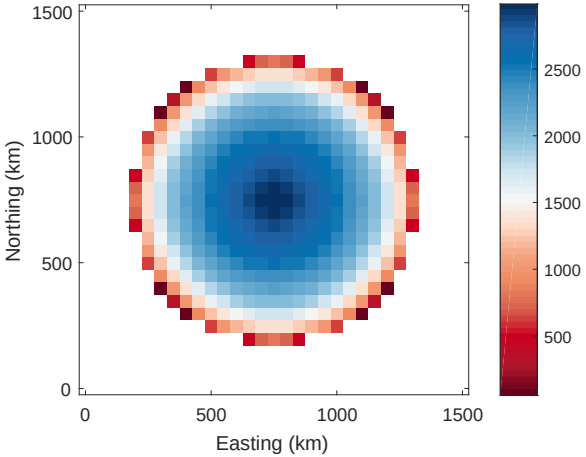

Modelled ice thickness according to the EISMINT-MM experiment.

A Greenland SIA ice sheet model

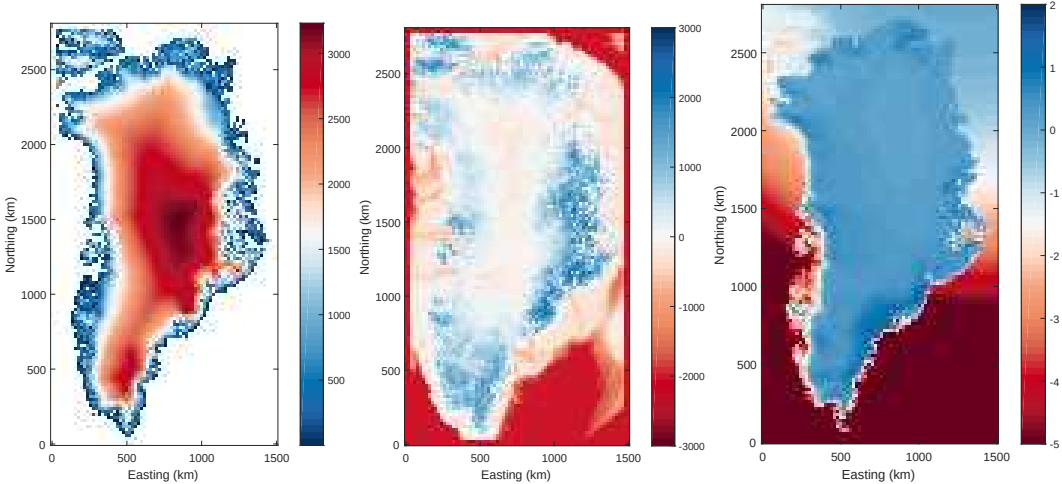

Observed surface topography (left), bedrock topography (centre) and surface mass balance (right) for the Greenland ice sheet on a spatial resolution of 20km.

Model initialization

- Ice sheet spinup
  - Run ice sheet (with thermodynamics) in steady state under present-day conditions;
  - Force ice sheet with glacial-interglacial cycle until present-day;
  - In both case it results in an ice sheet that is thermo-mechanically sound, but ice geometry may differ from present-day.
  - Long time scales
- Inversion methods
  - Minimize difference between observed and modelled ice velocities for present-day geometry;
  - Optimize basal friction and/or ice stiffness
  - Not thermo-mechanically sound
  - Valid for short time scales
- Nudging methods
  - Minimize difference between observed and modelled ice thickness in transient run until steady state is reached
  - Optimize basal friction and/or basal melt/accretion (ice shelves)
  - Thermo-mechanically sound; modelled ice velocity not necessarily close to observed.

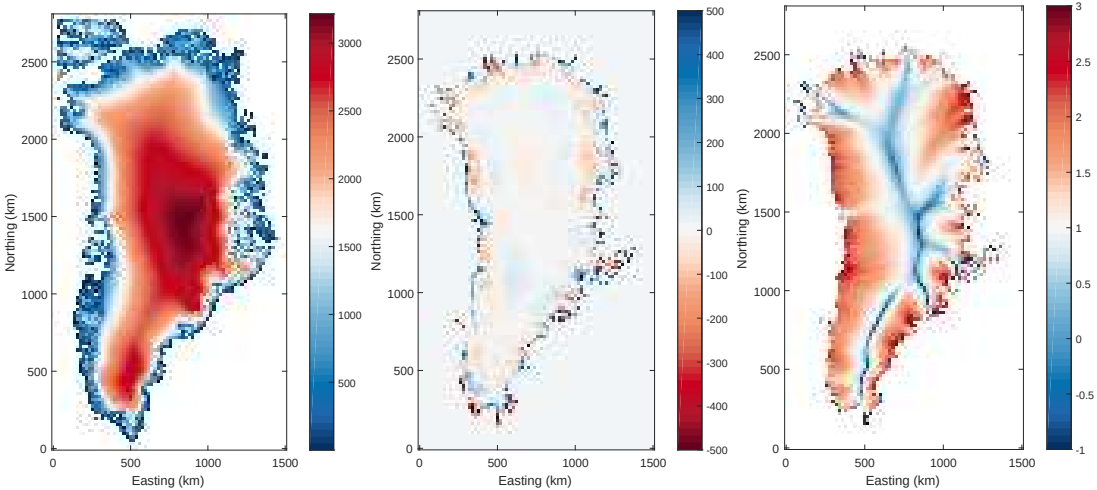

Steady-state modelled surface topography (left), difference between modelled and observed ice thickness (centre) and logarithmic vertical mean horizontal velocity (right) for the Greenland ice sheet on a spatial resolution of 20km after 20,000 years of integration, starting from present-day observed conditions.

Climate forcing of the Greenland model

$$T_s = T_s^{\text{obs}} - \gamma(h_s - h_s^{\text{obs}}) + \Delta T\,, \tag{100}$$

$$P = \dot{a}^{\text{obs}} \times 2^{(T_s - T_s^{\text{obs}})/\delta T}\,, \tag{101}$$

where $\gamma = 0.008°\text{C m}^{-1}$ is the lapse rate and δT is 10°C. A PDD model is used to determine surface melt rates,

$$\text{PDD} = \frac{1}{\sigma\sqrt{2\pi}} \int_0^A \left[\int_0^{\overline{T}+2.5\sigma} T \exp\left(-\frac{\left(T-\overline{T}\right)^2}{2\sigma^2} \right) \mathrm{d}T \right] \mathrm{d}t\,, \tag{102}$$

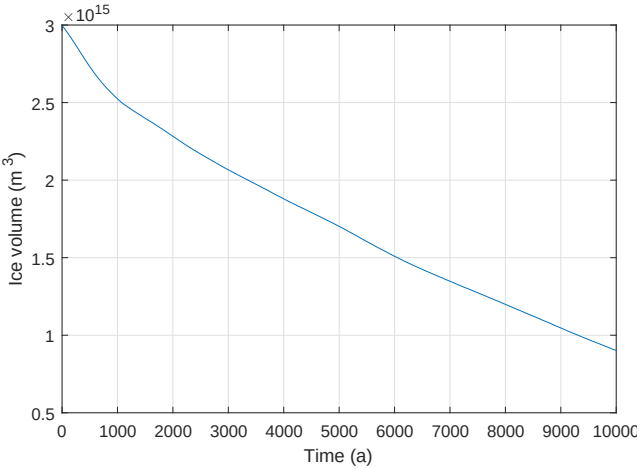

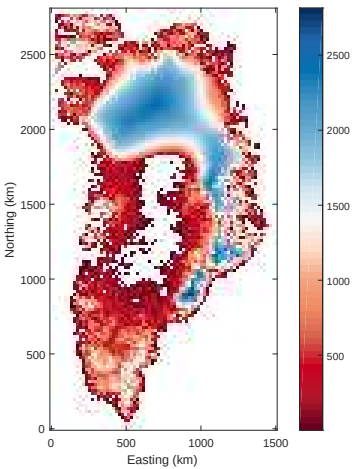

Evolution of the ice volume of the Greenland ice sheet when the SIA model is forced with a sudden background temperature change of $\Delta T = +5^{\circ}$C, correcting for the ice elevation-mass balance effect and using a PDD model for calculating surface melt (left). The right panel shows the ice sheet configuration after 10 000 years.

Numerical modelling of ice sheets and ice shelves

1. Commonly used approximations in ice flow modelling
2. Numerical modelling of ice sheets (SIA)
3. **Numerical modelling of marine ice sheets (SSA)**
   - Marine ice-sheet instability
   - Mathematical proof for MISI
   - A flowline SSA model with grounding line
   - Numerical solution to the ice-stream model
   - MISMIP experiments
   - Ice-shelf buttressing

Marine ice sheet dynamics

Fig. 3 *a*, Antarctic ice cover today, and *b*, after a 5–10 °C warming.

Mercer (1978) - Nature

Marine ice sheet dynamics

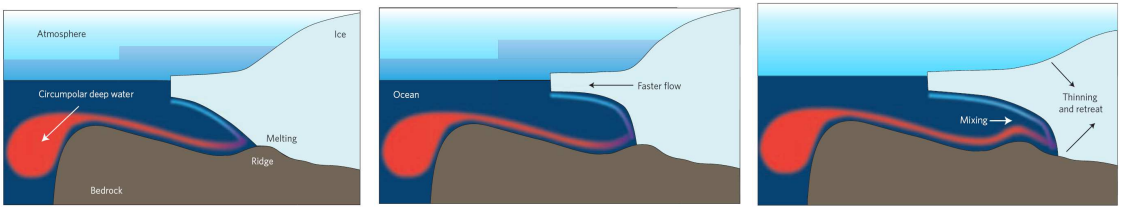

- Warm and deep circumpolar deep water (CDW) arrives on the continental shelf and reaches the grounding line.
- The grounding line is the basal contact between the ice sheet (or outlet glacier) and the ocean. It is the limit between the grounded ice sheet and the ice shelf.
- Warmer water provokes sub-ice shelf melt of several meters per year
- It leads to glacier thinning and acceleration as well as grounding line retreat.

Marine Ice Sheet Instability (MISI)

- Grounding line retreat provokes an increase in ice flux across the grounding line when the bedrock is downward sloping towards the interior.
- Consequence: sea level rise.
- MISI = due to grounding line retreat, ice thickness increase, requiring an increase in ice flux at the grounding line.
- This leads to irreversible glacier thinning and grounding line retreat (until grounding line reaches upward-sloping bedrock).

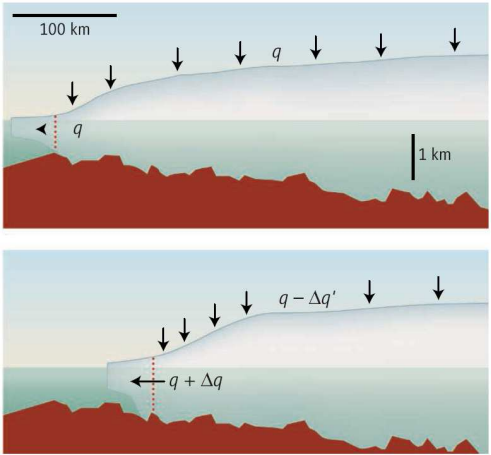

Mathematical proof for MISI (Schoof, 2007)

- Consider velocity boundary condition with the ocean:

$$4\eta h \frac{\partial u}{\partial x} = \frac{\rho g h^2}{2}\left(1 - \frac{\rho}{\rho_w}\right)$$

$$\eta = \frac{1}{2} A^{-1/n} \left(\frac{\partial u}{\partial x}\right)^{\frac{1}{n}-1}$$

$$\tau_b = c u^{1/m} \approx \rho g h \frac{\partial h}{\partial x}$$

$$uh = q$$

- Consider q constant near the grounding line, so that $\frac{\partial q}{\partial x} \approx 0$, or

$$\frac{\partial u}{\partial x} h + \frac{\partial h}{\partial x} u = 0 \Rightarrow \frac{\partial u}{\partial x} = -\frac{q}{h^2} \frac{\partial h}{\partial x}$$

- Combine with friction law

$$\frac{\partial u}{\partial x} = -\frac{c}{\rho g}\frac{q^{1+1/m}}{h^{3+1/m}}$$

- Boundary condition with ocean combined with η

$$4\eta h\frac{\partial u}{\partial x} = 2A^{-1/n}h\left(\frac{\partial u}{\partial x}\right)^{1/n} = \frac{1}{2}\rho g h^2\left(1-\frac{\rho}{\rho_w}\right)$$

- Replace velocity gradients by the friction law leads to an expression of flux q at the grounding line

$$q = \left(\frac{A(\rho g)^{n+1}(1-\rho/\rho_w)^n}{4^n c}\right)^{\frac{m}{m+1}} h^{\frac{m(n+3)+1}{m+1}}$$

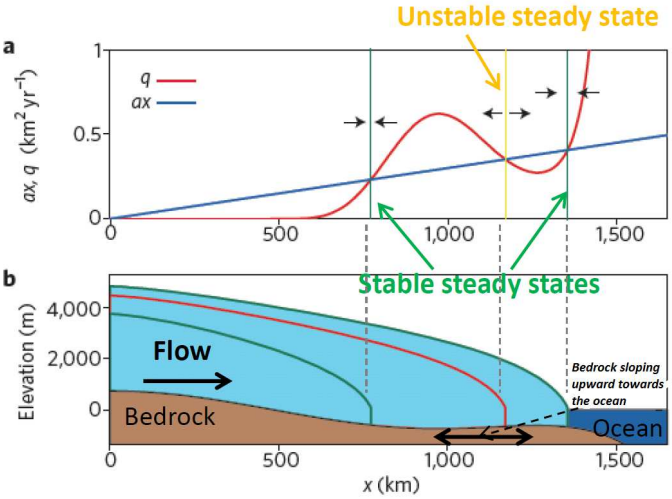

$$\frac{\partial h}{\partial t} = \dot{a} - \frac{\partial (uh)}{\partial x} = 0$$

$$\Rightarrow q = \dot{a}x$$

- Valid in absence of buttressing (plane strain)
- According to the bedrock profile, several equilibria are possible.
- Stable: for negative bed slope; Unstable: for positive bed slope (case for the West-Antarctic ice sheet).

Grounding-line theory: unbuttressed case

- Schoof (2006, 2007) qualitatively confirms Weertman (1974); Thomas and Bentley (1978)
- **GL is free boundary problem**: two independent conditions at moving boundary (one of which is flotation criterion)
- Depth-integrated longitudinal stress should balance on both sides of GL
- **MISMIP**: Marine Ice Sheet Model Intercomparison (Pattyn et al., 2012, 2013)
- To resolve GLs in numerical ice sheet models, a **high spatial resolution** is required (order of 100s of meters) otherwise behaviour is a numerical artefact (also depends on amount of sliding)

A flowline SSA model with grounding line

Consider a flowline and plain strain. Hence, all terms involving y are dropped.

$$4\frac{\partial}{\partial x}\left(\eta h\frac{\partial u}{\partial x}\right) - \beta^2 u = \rho_i g h\frac{\partial s}{\partial x} \tag{103}$$

where the effective viscosity η, neglecting lateral strain rates, becomes

$$\begin{aligned}\eta &= \frac{1}{2}A^{-1/n}\dot{\varepsilon}^{\frac{1-n}{n}} \\ &= \frac{1}{2}A^{-1/n}\left(\dot{\varepsilon}_{xx}^2\right)^{\frac{1-n}{2n}} \\ &= \frac{1}{2}A^{-1/n}\left|\frac{\partial u}{\partial x}\right|^{\frac{1-n}{n}}\end{aligned} \tag{104}$$

where β^2 is the basal friction of the ice stream

Sliding law

For a Weertman sliding law according to

$$u = A_s \tau_b^m \tag{105}$$

the value of β^2 in the ice stream is then defined as

$$\beta^2 = A_s^{-1/m} |u|^{1/m-1} \tag{106}$$

where $m = 3$ and A_s a sliding enhancement factor.

Numerical solution to the ice-stream model

We discretize (103) and (104) on a staggered grid, where the u-velocities are inbetween grid points (u_i lying between h_i and h_{i+1}). The effective viscosity η is calculated on the h-grid. By definition, we then have:

$$\eta_i = \frac{1}{2} A^{-1/n} \left| \frac{u_{i+1} - u_i}{\Delta x} \right|^{\frac{1-n}{n}} \tag{107}$$

The discretization of (103) then becomes

$$\begin{aligned} u_{i-1} \left\{ \frac{2(\eta_i h_i + \eta_{i+1} h_{i+1})}{(\Delta x)^2} - \frac{\eta_{i+1} h_{i+1} - \eta_{i-1} h_{i-1}}{(\Delta x)^2} \right\} \\ + u_i \left\{ -\frac{4(\eta_i h_i + \eta_{i+1} h_{i+1})}{(\Delta x)^2} - \beta_i^2 \right\} \\ + u_{i+1} \left\{ \frac{2(\eta_i h_i + \eta_{i+1} h_{i+1})}{(\Delta x)^2} + \frac{\eta_{i+1} h_{i+1} - \eta_{i-1} h_{i-1}}{(\Delta x)^2} \right\} \\ = \rho g \left(\frac{h_i + h_{i+1}}{2} \right) \frac{s_{i+1} - s_i}{\Delta x} \end{aligned} \tag{108}$$

Boundary conditions

Ice divide:

$$u = 0$$

Seaward edge:

$$\begin{aligned} 2\eta h \left(2\frac{\partial u}{\partial x}\right) &= \frac{\rho g h^2}{2}\left(1-\frac{\rho}{\rho_w}\right) \\ 2A^{-1/n} h \left|\frac{\partial u}{\partial x}\right|^{\frac{1-n}{n}} \frac{\partial u}{\partial x} &= \frac{\rho g h^2}{2}\left(1-\frac{\rho}{\rho_w}\right) \\ \frac{\partial u}{\partial x} &= A\left[\frac{\rho g h}{4}\left(1-\frac{\rho}{\rho_w}\right)\right]^n \end{aligned}$$

A numerical solution for the velocity on the last grid point is then given by:

$$u_N = u_{N-1} + A\left[\frac{\rho g h_N}{4}\left(1-\frac{\rho}{\rho_w}\right)\right]^n \Delta x$$

Boundary conditions

Lower boundary condition

$$h^\star = b - Z_{\text{sealevel}} + h\frac{\rho_i}{\rho_w}$$

so that the ice sheet is grounded for $h^\star > 0$ and floated otherwise.

$$\beta^2 = A_s^{-1/m} u^{1/m-1} \quad \text{for} \quad h^\star > 0$$
$$\beta^2 = 0 \quad \text{for} \quad h^\star \leq 0$$

Continuity equation

For ice streams and ice shelves, the continuity equations is not written as a diffusive equation but kept purely advective, so that,

$$\frac{\partial h}{\partial t} = \dot{a} - \frac{\partial}{\partial x}(uh) \tag{109}$$

For a semi-implicit scheme with u velocities on a staggered grid, the discretization of (109) becomes

$$h_{i,t+1} + \frac{(h_{i+1,t+1} + h_{i,t+1})u_i - (h_{i,t+1} + h_{i-1,t+1})u_{i-1}}{2\Delta x} = h_{i,t} + \dot{a}_i \Delta t \tag{110}$$

which is again solved as a tridiagonal system.

Example

We define a linearly-sloping bed along our flow-line, defined by $b(x) = x^{-1}$, where x is the horizontal distance (in km) and b the bed elevation (m a.s.l.).

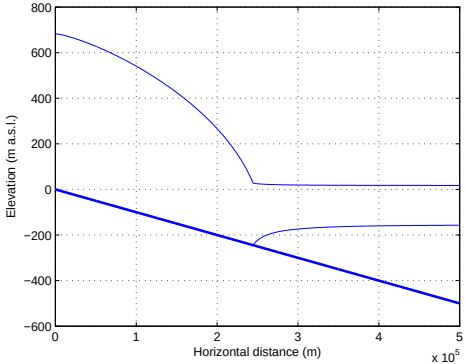

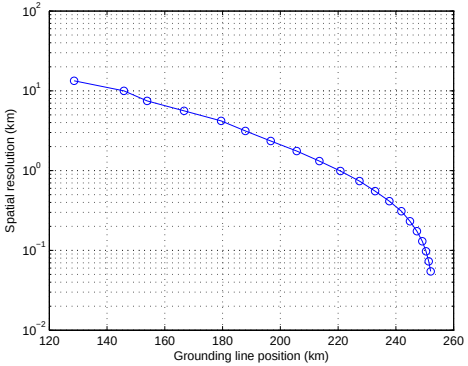

Left: surface, ice bottom and bedrock profiles for the ice stream and ice shelf according to the numerical model. Spatial discretization was taken as 250 m. Right: steady-state grounding line position as a function of spatial model resolution.

MISMIP experiments

Experiment 1: linearly sloping bedrock

$$b(x) = -100 - x\,, \tag{111}$$

Experiment 2: overdeepened bed

$$b(x) = 729 - 2184.8 \times \left(\frac{x}{750\text{ km}}\right)^2 + 1031.72 \times \left(\frac{x}{750\text{ km}}\right)^4 - 151.72 \times \left(\frac{x}{750\text{ km}}\right)^6 . \tag{112}$$

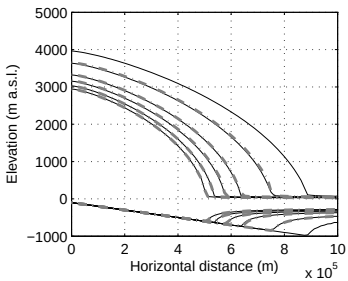
Elevation (m a.s.l.)
Horizontal distance (m)
x 10^5

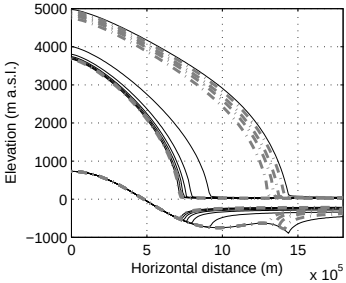
Elevation (m a.s.l.)
Horizontal distance (m)
x 10^5

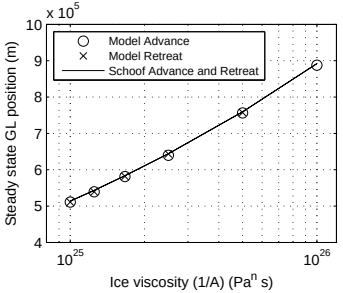
Model Advance
Model Retreat
Schoof Advance and Retreat
Steady state GL position (m)
Ice viscosity (1/A) (Pa^n s)
x 10^5

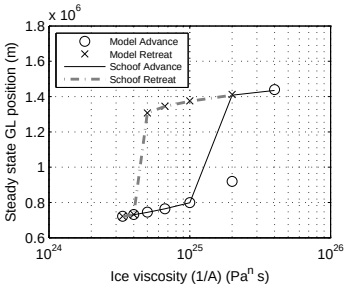
Model Advance
Model Retreat
Schoof Advance
Schoof Retreat
Steady state GL position (m)
Ice viscosity (1/A) (Pa^n s)
x 10^6

A) Antarctic bed topography

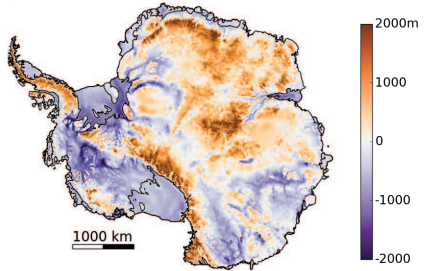

B) Unstable bed conditions

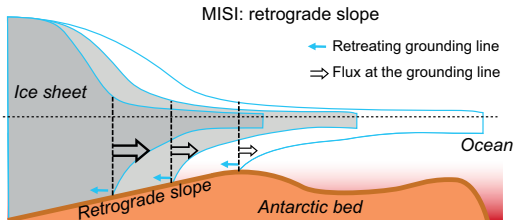

C) Coulomb/Weertman friction laws

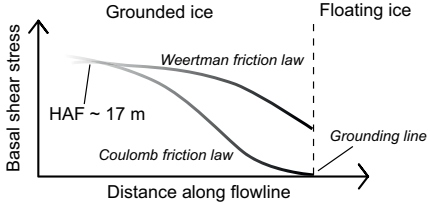

MICI: pro/retrograde slopes

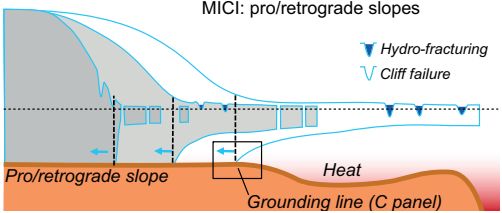

Ice-shelf buttressing

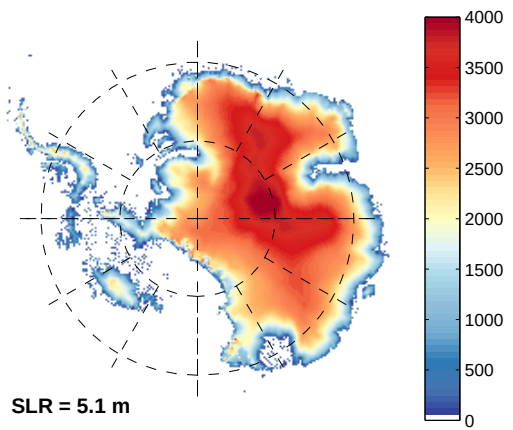

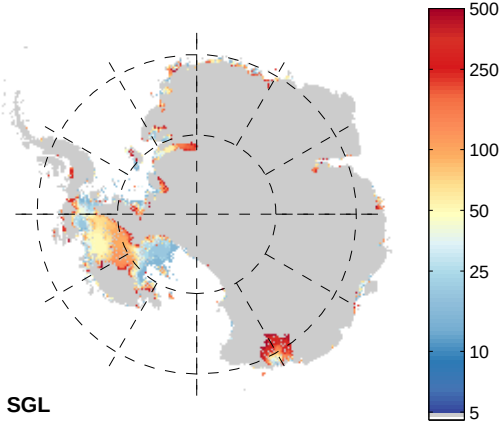

Left: Grounded ice sheet surface elevation (m a.s.l.), 500 years after sudden removal of all ice shelves. Right: grounding-line position in time according to the same experiment (colour scale is nonlinear and represents time in years). SLR denotes the contribution to sea level rise after 500 years (Pattyn, 2017).

Conclusions

- Ice sheet modelling has seen a tremendous evolution, from large-scale SIA to complex full-Stokes models
- Different ice-sheet models of varying complexity are now freely available for use (BISICLES, Elmer/Ice, ISSM, PISM, SICOPOLIS, ...): positive evolution, with pitfalls
- Complex models not necessarily better models
- For marine boundaries (grounding lines) high spatial resolution is required (<500 m)
- Time scales are also important (thermomechanical effects)
- Boundary conditions should be carefully analysed and taken into account properly
- The choice of model is function of what problem you want to study
- Interpretation of model results should be done with great care (as a function of the approximations made)